

# Morphology of zinc oxide thin films deposited by spray pyrolysis

ALİ OĞUZ ER, ASHRAF HASSAN FARHA<sup>a</sup>, CEBRAİL GÜMÜŞ<sup>b</sup>, EMİNE GÜNERİ<sup>c</sup>, YÜKSEL UFUKTEPE<sup>b\*</sup>

*Department of Physics, Old Dominion University, Norfolk, VA 23529, USA*

<sup>a</sup>*Electrical and Computer Engineering, Old Dominion University, Norfolk VA 23529, USA*

<sup>b</sup>*Department of Physics, Cukurova University, Adana, 01330, Turkey*

<sup>c</sup>*Department of Primary Education, Erciyes University 33039 Kayseri, Turkey*

The effect of deposition temperature on the surface morphology and optical properties of zinc oxide (ZnO) thin films were studied. The ZnO films were deposited on microscopic glass substrates using the spray pyrolysis method for different substrate deposition temperatures. The deposited films were characterized by an X-ray diffractometer (XRD), a spectrophotometer, scanning electron microscopy (SEM), and atomic force microscopy (AFM). The transmittance spectra recorded through the spectrophotometer exhibits 85% transmittance. The XRD spectra showed polycrystalline nature of ZnO film. Surface parameters were calculated and compared for different thin films. It showed that the films were polycrystalline with hexagonal wurtzite structure and *c*-axis was perpendicular to the substrate. The grain size of the films changed from 240 to 440 nm with different substrate temperatures. The optical energy gap of thin films increases from 3.26 eV to 3.35 as the substrate temperature increasing from 660 K to 700 K. It was found that growth temperature has significantly affected the morphological (grain size, surface roughness) as well as optical properties of ZnO films, which are extremely important as they can improve or degrade the device performance.

(Received November 11, 2011; accepted November 23, 2011)

**Keywords:** ZnO, Spray pyrolysis, Thin films, Surface morphology, Optical properties

## 1. Introduction

As a direct wide band gap (~3.37 eV) semiconductor with a large excitons binding energy (~59 meV), ZnO is one of the transparent conducting oxides whose thin films are important components in most thin film solar cells which have been investigated for many decades [1-5]. The study and growth of this material have been revisited in the past ten years because of its attractive fundamental properties and numerous applications, such as solar cells, transparent electrodes and light emitting devices, coatings, pigments in paints, and varistors [6, 7]. It also has other unique properties like non-toxicity, good piezoelectric behavior, and cost effectiveness.

Different techniques have been used to obtain ZnO thin films for these important applications such as chemical vapor deposition [8], radio frequency magnetron sputtering [9], molecular beam epitaxy [10], spray pyrolysis [11], and pulsed laser deposition [12]. A simple cost-effective method of deposition is highly desirable. Among the methods to prepare ZnO thin films, spray pyrolysis appears to have a great potential due to low cost and easily controllable deposition parameters, and it is easy to include in an industrial production line. Previously the optical, structural, and electrical characteristics of ZnO have been reported [13-15]. However, the surface morphology of ZnO films was not completely revealed. For device applications, it is essential to have a thorough understanding of the growth mechanism and morphology of ZnO. Surface morphology of thin film strongly depends

on the preparation conditions. The different surface morphology can be created by many techniques and often is characterized in terms of root mean square (RMS) roughness and grain size.

The main goal of our study was to monitor changes in ZnO surface morphology at different substrate temperature, while keeping all other parameters identical. For ZnO applications, it is of utmost importance to perform accurate characterization of optical properties such as refractive index, surface roughness, and morphology. In this work, the optical and morphological properties of ZnO thin films were investigated by means of X-ray diffraction (XRD), atomic force microscopy (AFM) and scanning electron microscopy (SEM).

## 2. Experimental details

ZnO thin films were prepared on glass substrates by spray pyrolysis technique [16]. The spray solution was 0.2 M Zn(CH<sub>3</sub>COO)<sub>2</sub>·2H<sub>2</sub>O (zinc acetate), isopropyl alcohol and distilled water (volume ratio 3 to 1). The carrier gas (compressed air) and solution were fed into a spray nozzle at a pre-adjusted constant atomization pressure. The flow rate of solution was 8 ml/min and the substrate temperature was held at 660 and 700 K. The variation in substrate temperature during deposition process was maintained within ± 5 °C. The nozzle to substrate distance was 30 cm and diameter of the nozzle was 0.3 mm. Commercial glass slides with the size of (76×26×1 mm<sup>3</sup>) were used as substrates.

The surface morphology of thin films was measured by using JEOL JSM-6060 LV SEM and Digital Instruments Dimension 3100 atomic force microscope. All AFM images were taken in air using tapping mode whereas SEM images were taken using a scanning electron microscope operated at an accelerating voltage of 30 kV. The structure and of ZnO films was analyzed by a Rigaku RadB X-ray diffractometer (XRD) with Cu  $K_{\alpha 1}$  radiation with  $\lambda = 1.54056 \text{ \AA}$  (30 kV, 15 mA, scanning speed =  $2^\circ/\text{min}$ ). The optical transmission of ZnO films were carried out with a double beam spectrophotometer (Perkin Elmer Lambda 2S) in the UV/VIS/NIR regions. The optical transmittance at normal incidence was recorded in the wavelength range of 300-1100 nm. The film thickness measurement was performed by a variable-wavelength and angle spectroscopic ellipsometer (Woollam M44). Thickness measurement was done at two angles  $67^\circ$  and  $71^\circ$ . Thickness for ZnO grown at 660 K was found to be  $\sim 680 \text{ nm}$  whereas it was  $\sim 540 \text{ nm}$  for film grown at 700 K.

### 3. Results

#### A. Surface morphology

Significant results of the effect of deposition temperature on the surface morphology and the optical constants of ZnO films have been reported here. In order to investigate the growth orientation and crystalline quality of ZnO, XRD was performed. Fig. 1 shows X-ray diffractograms for ZnO films deposited at 660 K and 700 K temperatures. The XRD pattern clearly showed the polycrystalline nature of the ZnO film, whose  $c$ -axis was oriented normal to the glass substrate. A strong peak appeared at the  $2\theta$  value of  $34.43^\circ$  denoting strong (002) orientation of crystalline film, the second peak of (101) showed less value of intensity at  $36.27^\circ$  [17]. However the (002) peak intensity increased with an increase in the deposition temperature. The growth of ZnO on glass substrate showed  $c$ -axis orientation; this phenomenon was also reported by the other chemical processes such as chemical bath deposition [18], sol gel [19], or spray pyrolysis method [20].

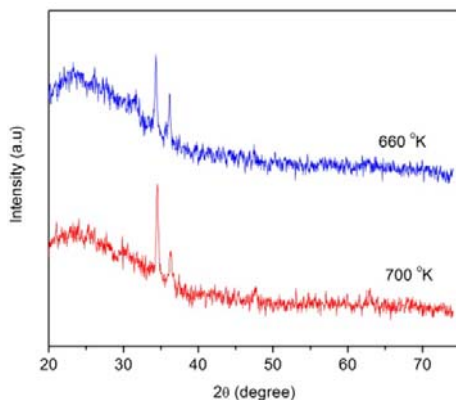


Fig. 1. XRD patterns of ZnO thin films deposited onto glass substrate at different temperatures.

The average crystallite sizes of the films deposited at different substrate temperatures have been calculated using the Scherrer's formula [21]:

$$D = \frac{0.97\lambda}{\beta \cos \theta} \quad (1)$$

where  $\lambda$  and  $\beta$  are the x-ray wavelength ( $1.54056 \text{ \AA}$ ) and the full width at half maxima (FWHM) of the XRD peak, respectively.

The lattice constant of the ZnO has been estimated from the XRD peaks shown in Fig. 1. The X-ray diffraction peak is observed when the Bragg condition is satisfied:

$$\lambda = 2d \sin \theta \quad (2)$$

where  $\lambda$  is the X-ray wavelength ( $\lambda = 0.1541 \text{ nm}$ ),  $\theta$  is the Bragg angle at which one observes a diffraction peak,  $d$  is the distance between each adjacent crystal planes in the set ( $hkl$ ) and can be found for the hexagonal phase from the following equation [21].

$$\frac{1}{d_{hkl}^2} = \frac{1}{3} \left( \frac{h^2 + hk + k^2}{a^2} \right) + \frac{l^2}{c^2} \quad (3)$$

where  $a$  and  $c$  are the lattice constants. The average crystallite sizes and lattice parameters from the XRD peaks were calculated from equation (1) and (3) and shown in Table 1. The obtained  $c$  and  $a$  values are in good agreement with the standard data [17]. The calculated values of the average crystallite sizes are in the nanometer range and **change** with deposition temperature, the size of the both (002) and (101) oriented grains in the film increases with deposition temperature. The increase in the crystallite size with increasing the substrate temperature can be explained due to the merging of the smaller particles into larger ones and is a result of potential energy difference between small and large particles and can occur through solid-state diffusion [22, 23].

Table 1. Variation of film thickness, particle size, and lattice parameters with substrate temperature.

Substrate temperature (K)	Film Thickness (nm)	Lattice parameters		Average crystallite size (nm)
		a(Å)	c(Å)	
660	680	3.248	5.197	17.18
700	540	3.247	5.202	27.78

In order to examine the surface of the films in detail, we have performed SEM and AFM measurements due to the fact that they are more sensitive to the surface structure. The SEM image of ZnO grown at 700 K, in Fig. 2(a), shows the non-uniform distribution of particles. We observe the non-uniformity in size and shape distribution as it will be confirmed by AFM images later. The corresponding AFM image ( $2.5 \times 2.5 \mu\text{m}^2$ ) of SEM, shown in Fig. 3(a), could be described as a collection of high density 3D clusters with different shapes, heights and

sizes. This type of AFM image is generally observed for heteroepitaxy structures at low temperatures. The majority of these islands are elongated pyramidal-shaped with a small fraction of colloidal particles. Average particle density is  $\sim 5.0 \times 10^9 \text{ cm}^{-2}$ . Particles can go up to  $\sim 75 \text{ nm}$  in height and  $\sim 440 \text{ nm}$  in size. The SEM image of ZnO film grown at 700 K was shown in Fig. 2(b). One can notice the uniformity of particles enhanced and size decreased by visual inspection. Fig. 3(b) shows AFM image for film grown at 700 K. It is clearly seen that the film at this temperature has lower island density,  $\sim 1.0 \times 10^9 \text{ cm}^{-2}$ , lower coverage ratio, smaller average grain size and height compared to the film grown at 660 K. AFM image at this condition reveals better crystalline structure and more uniform size distribution as also confirmed by SEM image in Fig. 2(b). Most of the islands are colloidal shape along with small number of elongated ones. The maximum height for these particles is as high as 60 nm and the maximum grain size is around  $\sim 240 \text{ nm}$ . These islands have higher aspect ratio compared to the film grown at 660 K. This shows that particles favor the growth in height rather than in size as we increase the growth temperature. Moreover, average lateral aspect ratio is smaller which also indicates that particles don't prefer to grow laterally.

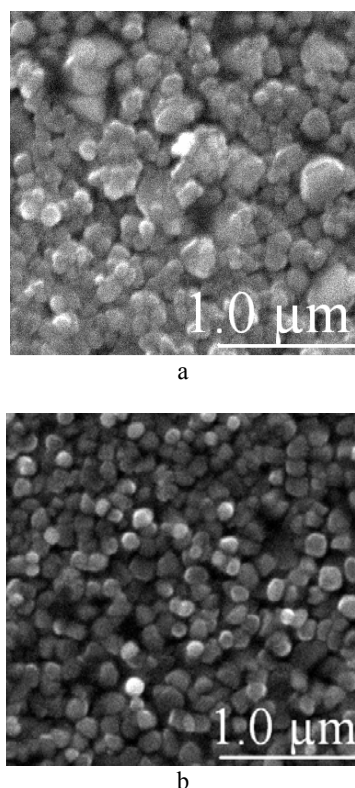


Fig. 2. SEM images with line scan of the ZnO films (a) grown at 660 K, (b) and 700 K.

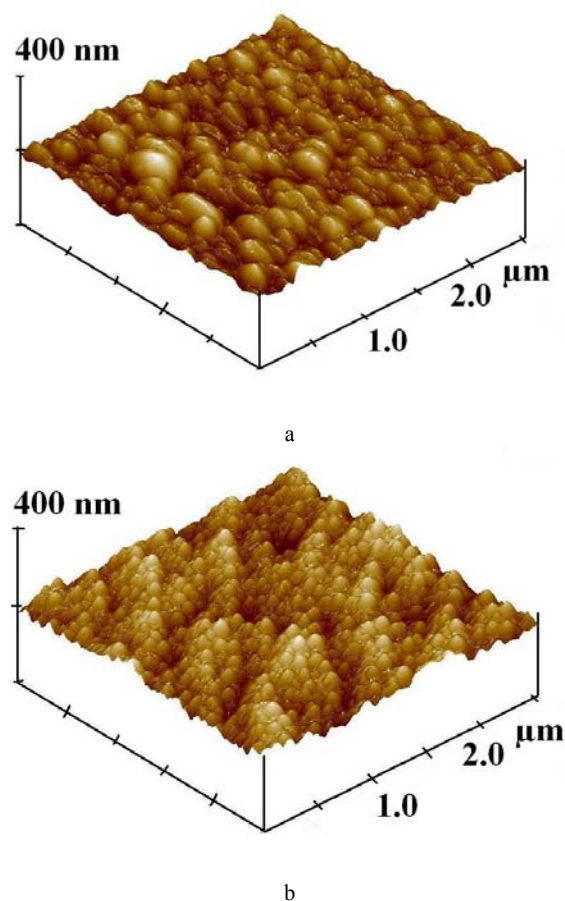
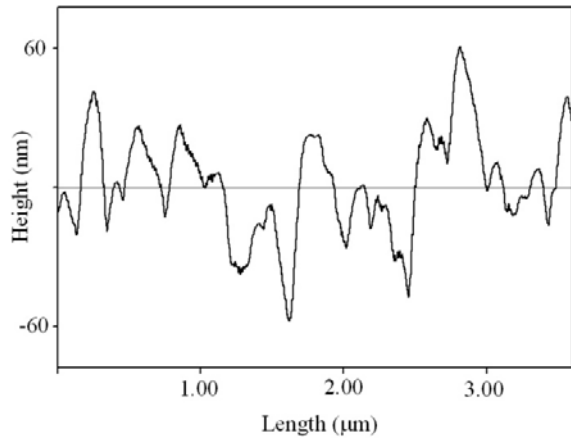
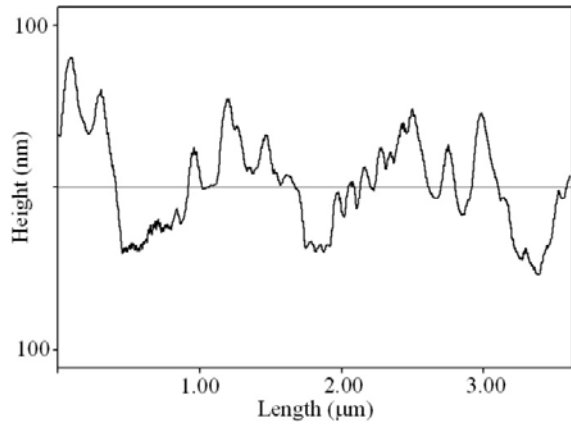


Fig. 3. Topographic image of AFM (a) grown at 660 °K (b) at 700 °K.

We performed AFM line scans on two ZnO samples. The result of AFM measurements on 660 and 700 K samples were analyzed by using Digital Instruments V5.31r1 software. AFM line scan measurements are shown in Fig. 4(a) and (b). The results show that mean surface roughness at 660 K film is  $\sim 13 \text{ nm}$  whereas that of 700 K is  $\sim 17 \text{ nm}$ . Therefore, we can say that the sample grown at 700 K has a slightly rougher surface compared to the sample grown at 660 K. Deposition on higher temperature substrate was significantly suppressed and the size of grains reduced from 440 nm to 240 nm. It was shown that roughness of ZnO films on glass substrate increase with an increase in the substrate temperature [24]. Line scans of AFM images reveals that the surface roughness increases as a result of grains decreasing. Higher temperature promotes the migration of the sputtered species at the surface and improves the film crystallinity. However, the film with higher grains during the low temperature growth process Zn creates new nucleation centers, which in turn change the nucleation type from homogeneous to heterogeneous, and deteriorates the crystal structure.



a



b

Fig. 4. Line scan of AFM images (a) grown at 660 °K (b) at 700 °K.

## B. Optical properties

Fig. 5 shows the optical transmittance spectra of ZnO thin films at 660 and 700 K depositions in the wavelength range from 300 to 1100 nm. The films are highly transparent in the visible range of the electromagnetic spectrum with an average transmittance values up to 85%. On the other hand, the transmission drops almost zero when the photon energy in shorter wavelength region. As seen from Fig. 5, the optical transmission edge is not significantly affected by the different deposition temperature at shorter wavelengths. The transmission of ZnO thin films deposited at higher temperature is significantly higher than the lower temperature growth due to different surface morphology.

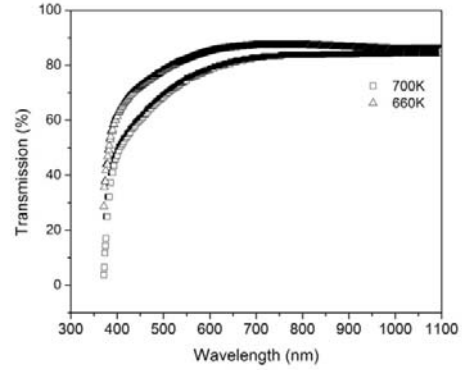


Fig. 5. Optical transmittance ( $T$ ) at normal incidence for two ZnO films grown at 660 °K and at 700 °K.

The optical properties of the films, such as refractive index ( $n$ ), absorption coefficient ( $\alpha$ ) and extinction coefficient ( $K$ ) were determined from a transmittance spectrum, using the relation between absorption ( $A$ ), transmission ( $T$ ) and the reflectance ( $R$ ) of the film [25].

$$R = 1 - T - A \quad (4)$$

The refractive index ( $n$ ) is calculated from the following equation;

$$n = \frac{1-R}{1+R} + \sqrt{\frac{4R}{(1-R)^2} - K^2} \quad (5)$$

The extinction coefficient  $K$  at given  $\lambda$  and is given by

$$K = \frac{\alpha \lambda}{4\pi} \quad (6)$$

If the thickness of the film  $t$  is known the absorption coefficient where  $\alpha$  can be obtained from the following equation:

$$\alpha = \frac{\ln(T)}{t} \quad (7)$$

At the beginning, equation (7) was used to calculate the absorption coefficients of the films. After that both  $A$  and  $K$  were derived from  $A = \frac{\alpha t}{2.303}$  equation, and equation

(6) respectively. Then the reflectance ( $R$ ) was calculated from equation (4). As the last step for the optical parameters, equation (5) was applied to get the refractive index of the films. The variations of refractive index  $n$  and extinction coefficient  $K$  with wavelength calculated from equation (5) and (6) and are shown in Fig. 6 (a) and (b). Fig. 6 (a) shows the calculated refractive index as a function of wavelength for two ZnO samples. The values of the refractive index at wavelength of 600 nm are 1.77 and 1.99 for films deposited at 700 and 660 K, respectively. The refractive index in the visible region decreased with the increase of the substrate temperature. These values are in same range of refractive index values obtained for ZnO films prepared by filtered vacuum arc deposition [26]. Our analysis shows that both refractive

index and the extinction coefficient are decreasing as the wavelength increase in the visible region.

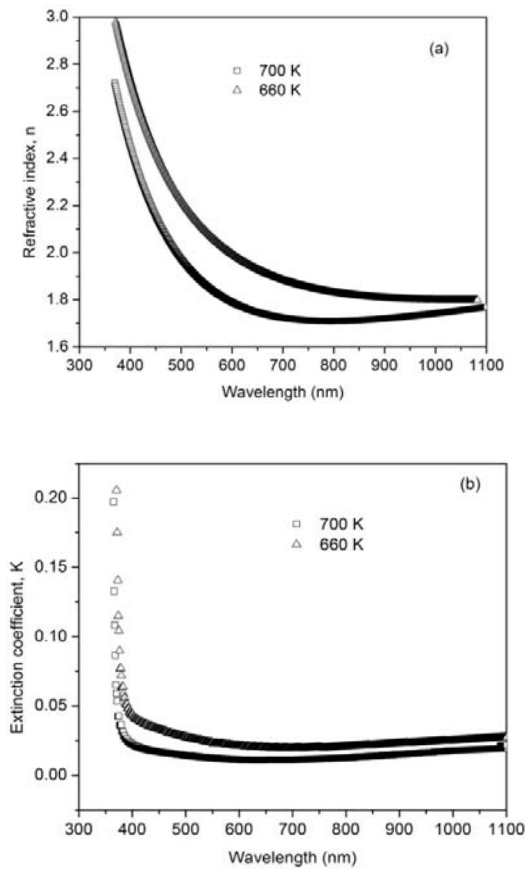


Fig. 6. Plots of optical constants versus wavelength: (a) of refraction index ( $n$ ) and (b) extinction coefficient ( $K$ ).

The optical absorption edge in semiconductors refers to an optical energy band gap between valence band and conduction band. According to Tauc's power law, the energy gap  $E_g$  of direct transitions is given by [27]:

$$(ah\nu) = B(h\nu - E_g)^{1/2} \quad (8)$$

where  $B$  is constant, the photon energy  $h\nu$  and the energy gap  $E_g$  are being expressed in eV. Fig. 7 shows the Tauc's plot of  $(ah\nu)^2$  versus photon energy for ZnO thin films. According to equation (8), the energy gap is calculated from extrapolation of the straight line (at high energy) on the photon energy axis. The value of  $E$  at this point defines the optical band gap energy,  $E_g$ . From figure 6 the energy band gap values are determined to be 3.26 eV and 3.35 eV for films grown at 660 K and 700 K, respectively. It was evident from Fig. 7 that the band gap increased with the increase in the deposition temperature, which could be due to smaller particle size. The band gap is more affected when the particles are smaller as the band gap varies approximately with inverse-square of the particle size [23]. The energy gap value increases with increasing the

deposition temperature of the film which is in good agreement with the literature [28,29]. Higher deposition temperature leads to the shift in the optical band absorption edge toward the bulk value of ZnO which is between 3.437-3.479 eV [30] which could be due to lesser defects and better crystal structure obtained at higher deposition temperature. It is important to control the size of the band gap of nanometer-sized semiconductor particles as potential amplifiers operating at 1.3 and 1.5  $\mu\text{m}$  wavelengths for telecommunication devices, which would be possible only by careful band-gap tuning [31,32].

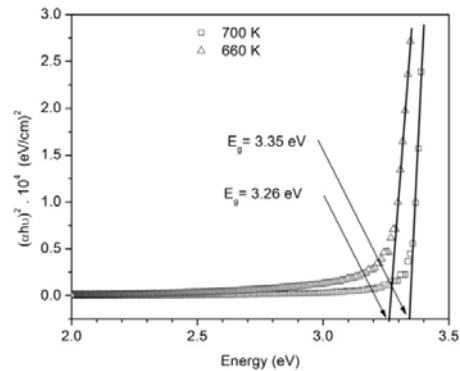


Fig. 7. Plots of  $(\alpha h\nu)^2$  versus the photon energy  $h\nu$  of the ZnO thin films of different deposition temperatures. The obtained values of the optical band gap are indicated with drawn lines.

Substrate temperature is considered as a major important parameter to determine the quality of thin films as it controls the atom mobility on the film surface. It was shown that there is a strong correlation between grain size and optical properties in ZnO thin films [33]. Influence of deposition temperature on ZnO properties have been studied by PLD between 25 and 500  $^{\circ}\text{C}$  [35] (grain size increases with temperature), by sol-gel method between 900-1200  $^{\circ}\text{C}$  [34], and between 300 and 600  $^{\circ}\text{C}$  [36], and by the r.f. magnetron sputtering method between 0 and 900  $^{\circ}\text{C}$ . It was found that grain size changes with temperatures in those studies. However, it was also shown that grain size was independent of temperature in the range of 420 K and 490 K [37]. Our results show that grain size decreases as we increase the substrate temperature. The reason could be the critical deposition temperature for epitaxial growth of ZnO could be  $\sim 600$  K. In that case, clusters with large grain size is expected since surface diffusive species are less mobile and they don't have enough kinetic energy to reach suitable growth site. Once enough diffusion energy is provided by increasing substrate temperature, those species will gain acceleration and have enough energy to diffuse more and epitaxial growth, resulting smaller grain size, will be observed. As a result smoothness, C-axis orientation of film has been observed, which has been indicated by the increase of peak strength and decrease of full-width at the half-maximum (FWHM) value, as could be seen in XRD images in Fig. 1.

Moreover, it should be kept in mind that, for every deposition rate, there exists an optimum growth temperature.

#### 4. Conclusion

We studied the effects of the growth temperature on surface morphology and optical properties of ZnO films grown on glass substrate at 660 and 700 K by spray pyrolysis method. The deposited films at both temperatures exhibit excellent crystalline structure with (002) preferential orientation. The surface morphology was found to change significantly with growth temperature. ZnO film grown at 660 K is less rough than that grown at 700 K. The roughness of the films results as formation of a micro-grain surfaces were found for higher growth temperatures. The size of grains decreased with increasing growth temperature, from about 440 nm to 240 nm and as results of that the surface roughness increases, the crystalline and optical quality became better. The optical band gap of ZnO films shows a small increase from 3.26 eV to 3.35 eV as deposition increases. It was clearly observed that deposition temperature can change the surface structure and surface morphology significantly and the optical properties of ZnO films were dependent significantly on the surface morphology.

#### References

- [1] G. J. Exarhos, X. D. Zhou, *Thin Solid Films* **515**, 7025 (2007).
- [2] M. Grätzel, *Nature* **414**, 338 (2001).
- [3] A. Ashrafi, C. Jagadish, *Journal of Appl. Phys.* **102**, 071101 (2007).
- [4] K. Ellmer, A. Klein, B. Rech, (ed) Springer-Verlag Berlin 2008.
- [5] A. Janotti, C. G Van de Walle, *Rep. Prog. Phys.* **72**, 126501 (2009).
- [6] C. Jagadish, S. J. Pearton, (ed) New York: Elsevier 2006.
- [7] Y. Huang, X. F. Duan, Y. Cui, L. J. Laudon, K. H. Kim, C. M. Lieber, *Science*, **294**, 1313 (2001).
- [8] J. Garnier, A. Bouteville, J. Hamilton, M. E. Pemble, E. Martyn, I. M. Povey, M. Ian, *Thin Solid Films*, **518**, 1129 (2009).
- [9] L. P. Peng, L. Fang, X. F. Yang, Y. J. Li, Q. L. Huang, F. Wu, C. Y. Kong, *J. of Alloys and Comp.* **484**, 575 (2009).
- [10] M. S. Kim, T. H. Kim, D. Y. Kim, G. S. Kim, H. Y. Choi, M. Y. Cho, S. M. Jeon, J. S. Kim, J. S. Kim, D. Y. Lee, J. S. Son, J. I. Lee, J. H. Kim, E. Kim, D. W. Hwang, J.Y. Leem, *J. Crystal Growth*, **311**, 3568 (2009).
- [11] C. Gumus, O. M. Ozkendir, H. Kavak, Y. Ufuktepe, *J. Optoelectron. Adv. Mater.* **8**, 299 (2006).
- [12] G. M. Fuge, T. M. S. Holmes, M. N. R. Ashfold, *Chem. Phys. Lett.*, **479**, 125 (2009).
- [13] S. J. Pearton, D. P. Norton, K. Ip, Y. W. Heo, T. Steiner, *Prog. Mater. Sci.* **50**, 293 (2005).
- [14] G. J. Exarhos, X. D. Zhou, *Thin Solid Films* **515**, 7025 (2007).
- [15] J. Wei, B. Y. Man, M. Liu, C. S. Chen, A. H. Liu, L. B. Feng, *J. Optoelectron. Adv. Mater.* **11**, 1830 (2009).
- [16] J. B. Mooney, S. B. Radding, *Ann. Rev. Mater. Sci.* **12**, 81 (1982).
- [17] Powder Diffraction File 03-065-3411, International Center for Diffraction Data, PDF-2/Release 2004.
- [18] A. Drici, G. Djeteli, G. Tchangbedji, H. Derouiche, K. Jondo, K. Napo, J. C. Bernède, S. Ouro-Djobo, M. Gbagba, *Phys. Stat. Sol. (a)* **201**, 1528 (2004).
- [19] S. W. Xue, X. T. Zu, W. G. Zheng, H. X. Deng, X. Xiang, *Physica B* **381**, 209 (2006).
- [20] M. Krunks, T. Dedova, I. Oja Açıık, *Thin Solid Films* **515**, 1157 (2006).
- [21] B. D. Cullity, *Elements of X-ray Diffraction*, Addison-Wesley, New York, 1956.
- [22] K. K. Nanda, F. E. Kruis, H. Fissan, *Phys. Rev. Lett.* **89**, 256103 (2002).
- [23] K. K. Nanda, F. E. Kruis, H. Fissan, M. Acet, *J. Appl. Phys.*, **91**, 2315 (2002).
- [24] M. Sucheá, S. Christoulakis, M. Katharakis, G. Kiriakidis, N. Katsarakis, E. Koudoumas, *Appl. Surf. Sci.* **253**, 8141 (2007).
- [25] N. Benramdane, W. A. Murad, R. H. Misho, M. Ziane, Z. Kezzab, *Materials Chem. and Phys.* **48**, 119 (1997).
- [26] E. Çetinörgü, S. Goldsmith, R. L. Boxman, *Surf. and Coatings Techn.* **201**, 7266 (2007).
- [27] J. Tauc, *Amorphous and Liquid Semiconductors*, (1974) Plenum, New York.
- [28] P. Singh, A. Kumar, Deepak, D. Kaur, *J. of Crystal Growth*, **306**, 303 (2007).
- [29] U. Alver, T. Kılınc, E. Bacaksız, S. Nezir, *Materials Chem. and Phys.* **106**, 227 (2007).
- [30] O. Madelung (ed.) *Semiconductors other than Group IV Elements and III–V Compounds* (1992) Berlin: Springer.
- [31] S. B. Quadri, J. Yang, B. R. Ratna, E. F. Skelton, *Appl. Phys. Lett.* **69**, 2205 (1996).
- [32] J. Z. Jiang, L. Gerward, R. Secco, D. Frost, J. S. Olsen, J. Truckenbrodt, *J. Appl. Phys.* **87**, 2658 (2000).
- [33] T. Matsumoto, H. Kato, K. Miyamoto, M. Sano, E. A. Zhukovb, *Appl. Phys. Lett.*, **81**, 1231 (2002).
- [34] A. Og. Dikovska, P. A. Atanasov, C. Vasilev, I. G. Dimitrov, T. R. Stoyanchov, *J. Optoelectron. Adv. Mater.* **7**, 1329 (2005).
- [35] S. Y. Chu, T. M. Yan, S. L. Chen, *J. Mater. Sci. Lett.* **19**, 349 (2000).
- [36] Y. Zhang, W. Fa, F. Yang, Z. Zheng, P. Zhang, *Ionics* **16**, 815 (2010).
- [37] M. Janda, A. Kubov, *Kristall und Technik*, **11**, K53 (1976).